

Exploring the Dynamic Scheduling Space of Real-Time Generative AI Applications on Emerging Heterogeneous Systems

Rachid Karami¹, Rajeev Patwari², Hyoukjun Kwon¹, and Ashish Sirasao²

¹University of California, Irvine

²Advanced Micro Devices Inc.

Abstract

The integration of generative AI models, particularly large language models (LLMs), into real-time multi-model AI applications such as video conferencing and gaming is giving rise to a new class of workloads: real-time generative AI (RTGEN). These workloads combine the compute intensity and dynamic execution patterns of generative models with the stringent latency and concurrency constraints of real-time inference. To meet the diverse demands of RTGEN workloads, modern edge platforms increasingly adopt heterogeneous system-on-chip (SoC) architectures that integrate CPUs, GPUs, and NPUs. Despite the potential of heterogeneous SoC, the scheduling space complexity and performance implications of RTGEN workloads on such platforms remain underexplored.

In this work, we perform a comprehensive characterization of RTGEN workloads on AMD’s latest heterogeneous SoC, Ryzen AI. We construct realistic multi-model scenarios inspired by industry use cases and profile model performance across all available backends. Using this data, we evaluate five scheduling policies and their impact on both real-time metrics (e.g., deadline violation rate) and LLM performance (e.g., time-to-first-token and tokens-per-second). Our results show that scheduling decisions significantly affect workload performance (e.g., leading to a 41.7% difference in deadline violation rates on average), and highlight the need for scheduling strategies that are aware of workload dynamics and hardware heterogeneity. Our findings underscore the importance of workload-aware, dynamic heterogeneous scheduling in enabling high-performance, on-device RTGEN applications.

1. Introduction

The rapid advancement of artificial intelligence (AI) algorithm has successfully replaced many traditional algorithms with AI models such as those in computer vision [9, 23] and language processing [40]. Such a trend led to recent real-time applications such as augmented and virtual reality (AR/VR) that combine multiple AI models for complex application functionality [17]. One key trend today in such real-time multi-model AI workload is the inclusion of generative AI, which constructs real-time generative AI (RTGEN) workload. For example, Figure 1 (a) shows an example smart video conferencing application that utilizes a large language model (LLM) for real-time AI agent providing various functionalities such as summarization of the meeting and question answering based on the meeting context [46].

In addition to the large language model, other models such as image segmentation [44] for background blurring are simultaneously executed in a real-time manner. Such complex real-time AI workloads including generative AI models (i.e., RTGEN) lead to a major challenge to the AI system due to the heavy computation from generative AI and real-time requirement for other real-time AI models. Furthermore, emerging RTGEN applications [17] demonstrate heavy demands on the on-device processing for better privacy, model customization opportunities, and low response time.

To provide desired on-device AI performance for the RTGEN, a new class of hardware platforms that integrate CPU, GPU, and NPU (Neural processing unit; AI accelerator) in one system-on-chip (SoC) has emerged [4, 6, 33], as illustrated in Figure 1 (b). Such heterogeneous SoCs, such as AMD Ryzen AI [4], provide not only extra parallelization opportunities across NPUs and GPUs for multi-model workloads [16, 17] but also adaptivity to heterogeneous AI workloads in RTGEN. For example, in our evaluation, Llama3-1B’s prefill and decode stages are 64.7% faster on NPU and 81.5% faster on GPU, respectively.

Although the heterogeneous SoC demonstrated promising features for RTGEN, one major challenge is exponentially growing scheduling space (e.g., for our video conference scenario on a CPU + GPU + NPU system, the scheduling space size is $O(2^{125})$). In addition, the scheduling decision has a significant impact on the resulting computational performance. However, the scheduling space and resulting performance horizon have not been well-studied, which hinders high-performance on-device RTGEN on heterogeneous SoCs.

Therefore, in this work, we conduct a thorough performance characterization study of RTGEN on one of the latest heterogeneous SoC, AMD Ryzen AI [4]. For that, we first construct a realistic RTGEN workload scenarios inspired by real use cases from industry. Using the constructed workload scenarios, we conduct performance characterization of the usage scenarios on each backend on a heterogeneous SoC. Finally, we apply various scheduling policies and delve into their impact on the real-time performance (deadline violation rate) and LLM performance (time to first token and the number of tokens per second). Our characterization study shows that the impact of scheduling decision is significant (e.g., 41.7% difference in deadline violation rate, on average) and it is crucial to consider all the RTGEN’s

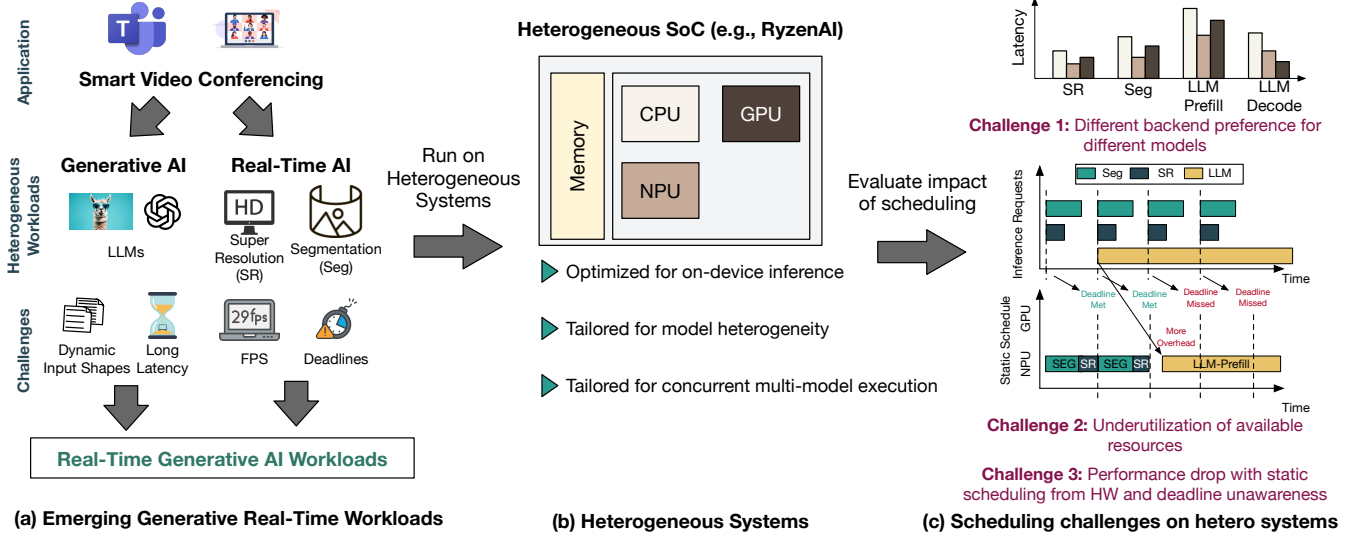


Figure 1: Challenges in scheduling emerging real-time - generative workloads on heterogeneous systems.

characteristics when we design a scheduler for *RTGEN*. Also, our study shows that heterogeneous backends provide superior real-time and LLM performance compared to a homogeneous SoC, which motivates further investigation of the optimization opportunity in the intersection of *RTGEN* and heterogeneous SoCs.

We summarize our contributions as follows:

- We define realistic *RTGEN* scenarios inspired by real-time applications integrating generative AI features, and highlight the challenges of this emerging class of multi-model workloads.
- We perform a workload characterization on a cutting edge heterogeneous platform, and show the importance of architectural heterogeneity for high performance deployment of *RTGEN* models on edge.
- We evaluate the impact of the scheduling policy on *RTGEN* workloads quantitatively, and highlight the scheduling challenges.
- We provide insights on the scheduling problem for *RTGEN* workloads running on heterogeneous systems.

2. Background and Motivation

2.1. Large Language Models

State-of-the-art large language models [1, 12, 42] (LLMs) are built by cascading multiple transformer blocks as shown in Figure 2 (a). Each transformer [40] block consists of a self-attention layer followed by a feed-forward layer. Given an input tensor X of size $S \times D$, where S is the length of the input sequence and D is the hidden dimension of the LLM, a transformer block first normalizes the input tensor and feeds the normalized tensor to the self-attention layer. The self-attention layer multiplies the normalized tensor by three weight matrices (W_Q, W_K, W_V) each of size $D \times D$

to generate the query Q , key K , and value V matrices of size $N \times D$. Then, the self-attention layer computes the attention scores by applying $\text{softmax}(QK^T)V$, and forwards the resulting tensor to the feed-forward layer.

Generative LLM inference consists of two main stages: *prefill*, and *decode* shown in Figure 2 (b). During the prefill stage, the LLM generates the first output token and populates the KV cache. The KV cache stores the K and V matrices of every processed token at every layer of the model. This common optimizations eliminates redundant K and V recomputation in the iterative decode stage. During the decode stage, the LLM auto-regressively generates new tokens. It uses the last generated token in the sequence and the KV cache entries of all the previous tokens to generate the next token.

Recently, LLMs have been integrating retrieval augmented generation (RAG) [7, 19] to augment the input context with relevant information retrieved from a database at real-time. Figure 2 (c) highlights the main components of a RAG pipeline: the encoder and the generator. The RAG pipeline pipeline’s encoder computes embeddings of the input prompt, and selects the top- K database entries that is the most similar to the input prompt. The input prompt is next augmented with the retrieved information and fed to the generator which is a LLM to generate the output response.

2.2. Real-Time Workloads

The success of ML models across computer vision and speech recognition tasks lead to an increased adoption of these models in various real-time applications [10, 17, 26, 46]. Video conferencing and gaming applications often integrate ML based features to improve the real-time user experience [10, 26, 39, 46]. For example, many video conferencing applications rely on segmentation DNNs to enable background blurring and customizations [21, 24, 26].

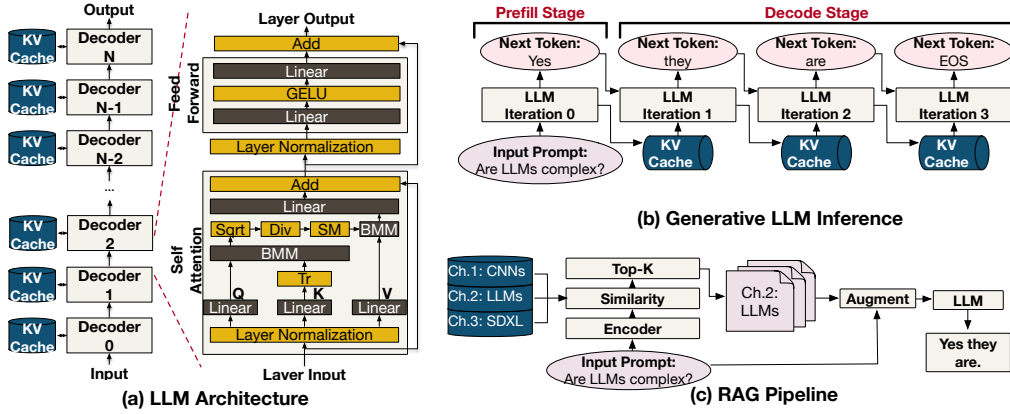


Figure 2: Overview of LLM architecture and generative inference.

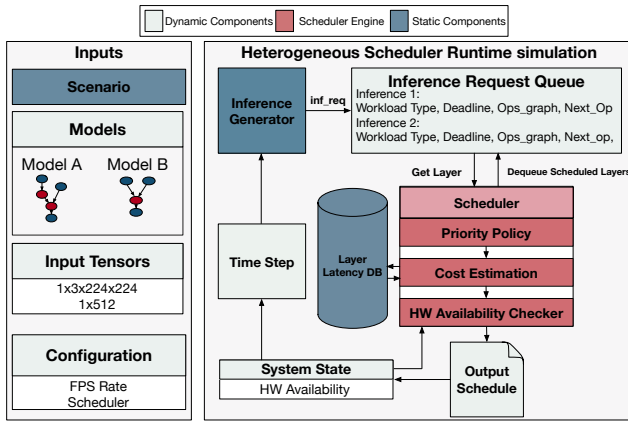


Figure 3: Overview of the runtime simulation used to evaluate the workloads scenarios defined in Table 2

These applications also use super-resolution networks [2, 28, 43] to improve the user’s quality of experience. This class of ML applications requires ML inference requests to be periodically serviced to provide a continuous and smooth user experience. Since the inference latency directly impact the user quality of experience, strict real-time processing requirements, quantified using the frame per second (FPS) processing rates, must be met.

2.3. Heterogeneous Systems

The heterogeneity in ML workloads paired with the increased demand of high performance inference lead to an increased adoption of heterogeneous systems to meet the computational and memory requirements of the inference workloads. Heterogeneous systems typically incorporate two or more distinct compute units (CPU, GPU, NPU).

CPU-GPU Systems. CPU-GPU systems comprise of a CPU connected to a discrete GPU via a PCI Express (PCIe) link. This type of heterogeneous systems is widely adopted across platforms from edge (e.g., laptops, workstations) to cloud devices. GPUs are widely adopted for deep learning

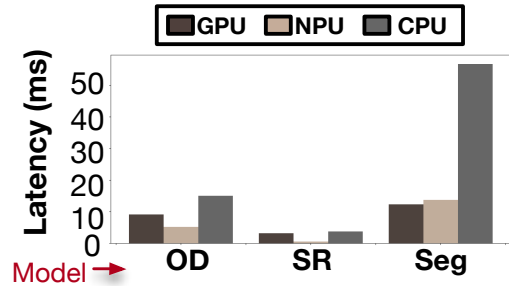


Figure 4: The impact of the hardware platform on the inference latency of selected real-time models.

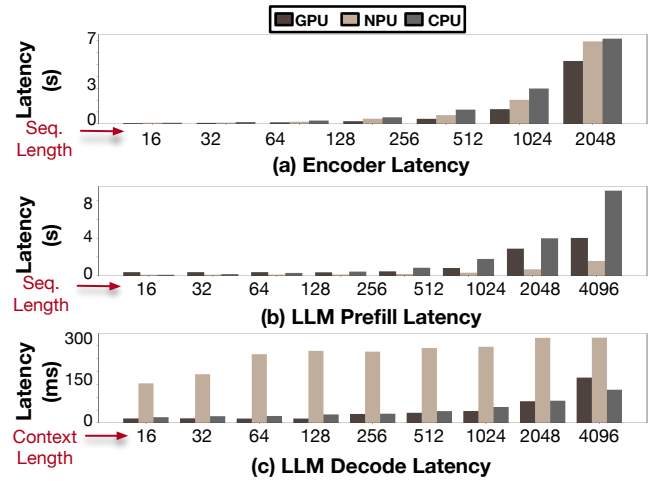


Figure 5: Comparing the latency of the (a) encoder, (b) prefill, and (c) decode stages of the RAG pipeline used in scenario A.

inference due to their high computational throughput. For instance, the AMD Radeon RX 7900 XTX offers up to 123 half precision TFLOPS [3]. However, GPUs consume significant amounts of energy, which poses a major challenge for power-constrained edge deployments [34].

Integrated Heterogeneous Systems. The increasing complexity and heterogeneity of machine learning workloads and the efforts to increase accessibility to GenAI have driven the development of tightly integrated heterogeneous platforms. Modern System-on-Chip (SoC) architectures, such as Apple’s M-series [6], AMD Ryzen AI [4], and Qualcomm Snapdragon [32], tightly integrate CPUs, NPUs, and GPUs on a single package. The tight integration of multiple compute engines unlocks potential opportunities for additional optimizations.

3. GenAI in Real-Time Applications

RTGEN workloads represent an emerging class of ML inference tasks that combine the challenges of generative and real-time models in a scenario-driven, multi-model setting. We outline the characteristics of multi-model *RTGEN* workloads and define four representative scenarios, summarized in Table 2, inspired by real applications.

3.1. *RTGEN* Characteristics

RTGEN workloads pose unique challenges due to the integration of generative LLMs with real-time, single- and multi-model inference workloads. Therefore, we define the following characteristics of emerging *RTGEN* scenarios: dynamic input shapes, real-time processing, multi-model execution, and model heterogeneity.

Dynamic Input Shapes. Generative LLMs in *RTGEN* scenarios process tensors with dynamic shapes, depending on the input sequence length and execution stage. During the prefill stage, the tensors have a $S \times D$ shape, S being the input sequence length and D the model’s hidden dimension. During the decode stage, the LLM auto-regressively generated a single token at a time by using inputs of shape $1 \times D$ in every decode iteration. The dynamically varying input sequence lengths of a generative LLM between the prefill and decode stages alter the LLM’s preferred backend. For instance, as shown in Figure 5, the LLM prefers the NPU during the compute-intensive prefill stage, but chooses the GPU for the memory- and bandwidth-intensive decode stage. As a result, static ahead-of-time (AoT) input-unaware scheduling will fail to capture input dynamicity leading to sub-optimal performance.

Real-Time Constraints. *RTGEN* applications include real-time tasks with strict frame rate requirements as shown in Table 2. Meeting these FPS targets is critical to maintaining quality of experience in applications such as real-time background blurring in video conferencing and resolution enhancement in gaming. Frame drops caused by missed deadlines directly degrade the user’s overall experience.

Multi-Model Execution. *RTGEN* scenarios require the execution of multiple models, often concurrently and in a cascaded manner. This concurrency can lead to dynamic backend availability, introducing significant challenges for scheduling—especially in the presence of models with dynamic tensor shapes.

Model Heterogeneity. *RTGEN* workloads deploy models from different task domains with diverse architectures. For

example, scenario B in Table 2 consists of a RAG and a super-resolution (SR) model. The RAG’s encoder and generator have both transformer based architectures, while the SR network is a convolutional neural network (CNN). This architectural diversity further complicates scheduling and backend selection.

3.2. Usage Scenarios

We use models from Table 1 to define four representative scenarios highlighted in Table 2, each inspired by practical edge AI applications.

Scenario A: AI Assistant. This scenario involves a RAG pipeline for text-based prompt answering. This scenario does not have real-time constraints, but it exhibits input dynamicity caused by the varying input prompt length of the RAG’s LLM.

Scenario B: Gaming I. This is a multi-model scenario that simulates a gaming scenario where the user interacts with a smart non-playable character [10, 31]. This scenario consist of a generative LLM and a SR network. The generative LLM pipeline drives the non-playable characters to converse with the user and answer their questions, and the real-time SR model improves the resolution of the game [2, 43].

Scenario C: Gaming II. This scenario represents a live-stream gaming session assistant. A segmentation model runs for background blurring and manipulation [?, 26, 41], while 2 super-resolution models runs to enhance the resolutions of the game [2, 43] and the streamed video [28]. A RAG based AI Assistant answers the user’s questions during the streaming process for a smoother experience [38].

Scenario D: Video Conference. The scenario describes a video conference call powered by a smart AI assistant [25, 46]. Scenario D deploys a RAG based assistant and includes a real-time segmentation model to support background blurring [26, 44], a real-time object detection (OD) model for gesture recognition [45], and a SR network for enhancing the quality of the video.

4. Methodology

4.1. Profiling Methodology

To profile the models in Table 1, we utilize the AMD open source RyzenAI SW [5]. The RyzenAI SW flow enables deploying models on both the NPU and the GPU of Ryzen AI processor described in Table 3, by leveraging the ONNX Runtime (ORT) [36] and the ONNX runtime generative AI (OGA) [27] inference frameworks. The RyzenAI SW toolchain utilize the VitisAI execution provider [29] for NPU deployment and the the DirectML execution provider [30] for GPU deployment.

To profile the LLM, the model is first quantized using the AWQ post-quantization [22] scheme to reduce the model’s weights to a 4 bit INT4 precision. Then, the quantized LLM graph is passed to the OGA runtime which partitions the LLM’s graph and maps it to the chosen backend (NPU or GPU). Afterwards we run the LLM for multiple input and output sequence lengths and record the latency of both the prefill and the decode stage.

TABLE 1: UNIT MODELS USED TO CONSTRUCT THE EVALUATED WORKLOAD SCENARIOS. TTFT, TPT, AND E2E REFER TO TIME TO FIRST TOKEN, TIME PER TOKEN, AND END-TO-END LATENCY RESPECTIVELY.

Application	Task	Models	Task Perf. Metric
Generative Agent	RAG Pipeline (RAG)	GTE Encoder [20]	TTFT, TPT, E2E
		Llama3-1B [12]	
	LLM	Llama3-1B [12]	
Background Blurring	Segmentation (Seg)	PointPainting [41]	Frame Drop Rate
Resolution Enhancement	Super Resolution (SR)	RCAN [43]	
Hand Gesture Detection	Object Detection (OD))	YOLOv3 [35]	

TABLE 2: DESCRIPTION OF THE REAL-TIME - GENERATIVE WORKLOAD SCENARIOS AND THEIR RESPECTIVE TARGET PROCESSING RATES IN FPS.

ID	Scenario	Tasks	Characteristics				Scenario Description
			Real-Time Processing	Dynamic Shapes	Multi-Model Exec.	Model-Heterogeneity	
A	AI Chatbot Assistant	RAG		✓		✓	RAG-based chatbot to answer the users prompts
B	Gaming I	LLM		✓	✓	✓	LLM-based non-playable characters
		SR	120 FPS				
C	Gaming II	RAG		✓	✓	✓	RAG-based game streaming assistant
		SR-120	120 FPS				
		SR-60	60 FPS				
		Seg	60 FPS				
D	Video Conference	RAG		✓	✓	✓	Video conference with RAG-based chatbot assistant
		SR	60 FPS				
		Seg	60 FPS				
		OD	60 FPS				

TABLE 3: HARDWARE PLATFORM CONFIGURATIONS USED FOR CASE STUDIES.

ID	CPU		NPU		GPU	
	Device	Memory	Device	TOPS	Device	TOPS
A	AMD Ryzen AI 9 365	24 GB	XDNA 2	50	AMD Radeon 880M	16

Similarly, we quantize the RAG’s encoder to BFloat16 and Float16 for NPU and GPU deployment respectively. We also quantize the SR, Seg, and OD networks to INT8. We then use ORT with the respective execution provider to run the quantized models and collect their inference latency. We use the collected latency profiles to drive Table 2’s scenarios simulation experiments.

4.2. Runtime Simulator

To evaluate the impact of scheduling on the performance of the emerging *RTGEN* workloads, we implement a Python-level simulator highlighted in Figure 3 to simulate the runtime of the different scenarios defined in Table 2 under the five scheduling policies described in Table 4. The simulator inputs consist of the scenario’s models, their input tensors, the real-time requirements (e.g. FPS), as well as a scheduling policy. Given those models, the inference generator issues inference requests based to the inference request queue based on each model FPS. Next, the scheduler module selects a layer or a model to be scheduled based on the system state, the cost of running the layer/model, and the selected scheduling policy. To estimate the deployment cost of every layer/model on a given backend, the scheduler relies on a latency database constructed using the latencies of the profiled models.

4.3. Scheduling Methodology

We evaluate the workload scenarios under the five scheduling policies listed in Table 4. To enable a structured

analysis of their trade-offs, we introduce the following taxonomy to captures the key features relevant to scheduling *RTGEN* workloads:

- **Deadline Awareness:** A scheduling policy is considered deadline-aware if it incorporates real-time constraints, such as frame rate deadlines, into its decision-making process.
- **Dynamic Hardware Selection:** A policy supports dynamic hardware selection if it determines the execution backend (NPU or GPU) at runtime, based on current system load and availability. This contrasts with ahead-of-time (AoT) policies that statically assign backends regardless of runtime conditions.
- **Heterogeneity Awareness:** A heterogeneous-aware policy is able to utilize multiple backends concurrently, taking advantage of both NPU and GPU resources to maximize parallelism and throughput.
- **GenAI Awareness:** GenAI-aware policies recognize the unique latency characteristics of generative models (e.g., LLMs) and ensures that long-latency models are not starved or preempted unnecessarily.

Each of the five scheduling policies differs in how it aligns with these taxonomy dimensions:

First-Come First-Serve AoT (FCFS-AOT). This policy schedules the next layer from the oldest inference request in the queue. The backend is selected statically ahead of time based on latency profiling. FCFS-AOT does not account for

TABLE 4: EVALUATED SCHEDULING POLICIES.

Scheduler	Deadline Aware	Dynamic HW Selection	Heterogeneity Aware	GenAI Aware
EDF-AOT	✓	✗	✓	✗
EDF-Dyn	✓	✓	✓	✗
FCFS-AOT	✗	✗	✓	✗
FCFS-Dyn	✗	✓	✓	✗
FTF	✓	✓	✓	✓

real-time deadlines, does not adapt to runtime hardware availability, and treats all models equally without regard to generative workloads.

First-Come First-Serve Dynamic (FCFS-DYN): Like FCFS-AOT, this policy schedules requests in arrival order, but it dynamically selects the backend at runtime based on current availability. It still lacks deadline awareness and does not distinguish between real-time and generative workloads.

Earliest Deadline First AoT (EDF-AOT): This policy prioritizes inference requests based on their deadlines, scheduling the layer from the request with the closest deadline. However, backend selection remains static and fixed prior to execution. While EDF-AOT introduces deadline awareness, it lacks both dynamic backend selection and GenAI-specific treatment.

Earliest Deadline First Dynamic (EDF-DYN): EDF-DYN improves upon EDF-AOT by choosing the execution backend dynamically at runtime. It retains the same deadline-aware behavior but adds runtime flexibility in hardware selection.

First Token First (FTF): FTF extends EDF-DYN with GenAI-specific enhancements. It prioritizes LLMs’ TTFT by treating the first token as a high-priority deadline, mitigating starvation during the compute-intensive prefill phase. Once the TTFT is served, FTF falls back to EDF-DYN behavior, since the decode stage latencies are more akin to the other non-generative models. This approach balances the stringent latency demands of real-time models with the long and stage-dependent latency of LLMs.

5. Case Studies

We begin by analyzing the performance of the models listed in Table 1. To collect performance data, we use ONNX Runtime Generative AI (OGA) for LLMs and ONNX Runtime (ORT) for all other models. The resulting profiling data populates the simulator’s latency database, which we use to simulate the workload scenarios from Table 2 and evaluate the impact of different scheduling strategies on *RTGEN* workloads running on emerging heterogeneous platforms.

5.1. Workload Characterization

We characterize the performance of the models in Table 1 and present the results in Figure 4 and Figure 5. As shown in Figure 4 and Figure 5, no single backend consistently offers the best performance across all models. **CNN-based Models.** The super-resolution (SR) network incurs the highest latency when executed on the CPU,

requiring 3.78 ms on average. Running the SR on the GPU reduces the inference latency by 14.6%. Nevertheless, deploying the SR network on the NPU achieves a significant speedup compared to the GPU and CPU. The NPU reduces the latency of the SR by 81.9% and 84.5% with respect to the GPU and CPU, and runs the SR inference in 0.59 ms on average.

A similar performance trend is observed for the object detection (OD) model. After NPU acceleration, the latency of the OD inference is 5.23 ms on average, a 42.9% and a 62.7% decrease compared to the GPU and CPU latencies. In contrast, the segmentation (Seg) model achieves its lowest latency on the GPU which is 10.2% faster than the NPU.

Transformer-based Models. In Figure 5, we observe that the encoder’s inference latency is the lowest for sequence lengths of 16 and 32 when the model is deployed on the NPU. The NPU latency is 31.9% and 10.9% lower than the GPU latency for an input sequence of length 16 and 32 respectively. As the sequence length increases, we notice that the NPU latency of the encoder becomes greater than the encoder’s GPU latency. At a sequence of 1024, the GPU inference latency is 22.3% lower than the NPU latency. These results indicate that the encoder’s optimal backend selection is input-dependent and varies with sequence length.

As for the LLM, we observe that the backend resulting in the lowest inference latency varies across the generation stages (prefill and decode). For the prefill stage, we notice in Figure 5 that running inference on the NPU results in an average speedup of $3.0\times$ across all input sequence lengths compared to running on the GPU. On the other hand, running the decode stage on the GPU results in a $7.5\times$ speedup over the NPU on average across varying context lengths. Since the prefill phase is a compute intensive stage and the decode phase is a memory and bandwidth (BW) intensive stage, the collected profiling data indicate the NPU is better suited for compute-bound workloads while the GPU is more suited for memory/BW-bound workloads on our evaluated system.

The profiling results reveal heterogeneity in backend preference both across different models and between stages of the same model.

This emphasizes the importance and advantages of heterogeneous platforms that provide multiple backend each tailored to a specific workload. Moreover, it indicates that heterogeneous systems are a great fit to run *RTGEN* workloads characterized by heterogeneous models.

5.2. *RTGEN* Scheduling

As discussed in Section 5.1, *RTGEN* models are heterogeneous and have diverse backend preferences. In addition, *RTGEN* workloads can exhibit dynamic behaviors due to dynamic input shapes, have strict deadlines, and run multiple models concurrently.

To evaluate how *RTGEN* workload characteristics interact with scheduling decisions on heterogeneous systems, we simulate four scenarios with five different scheduling policies. For every scenario, we analyze the models’ deadline violation rate, the LLM’s time-to-first-token (TTFT), and

its time-per-token (TPT). We present the results in Table 5. We also evaluate the effects of varying the input sequence length in Figure 6.

5.2.1. Scheduling Algorithm. For scenario A, we observe identical performance under all scheduling policies. This is expected because scenario A (AI chatbot assistant) does not have any real-time constraints. It also does not exhibit any model concurrency which simplifies the scheduling decision, because the RAG pipeline does not have to compete for resources with other models. Hence, the scheduling policy does not impact the performance of scenario A. On the other hand, the performance of the remaining scenarios is significantly affected by the scheduling policy.

Earliest Deadline. We notice that using an earliest deadline first (EDF) policy will always starve the generative LLM in all the workloads. EDF consistently prioritizes the model with the closest deadline, preempting LLM execution in favor of real-time tasks. For example, in scenario C, the EDF-AOT scheduler stops the LLM’s prefill execution to schedule the SR-120 on the NPU. This behavior leads to repeated preemption of the LLM, resulting in starvation and failure to complete execution. The case is similar for the EDF-DYN scheduler. Despite scheduling the models’ layers dynamically on the HW, it still prioritizes the model with the earliest deadline and schedules it on the best HW backend available. Since the latency of a single LLM layer in scenario C (98.62 ms) is larger than the largest frame duration (16.67 ms), the LLM will be stopped in favor of a model with a closer deadline, leading to the starvation of the LLM task. This indicates that *only considering deadline violation requirements greatly degrades the LLM’s performance.*

First Come First Serve. While servicing inference requests in arrival order improves the LLM’s TTFT and TPT relative to EDF strategies, it comes at the cost of increased deadline violations. We observe that applying a FCFS scheduler leads to a TTFT performance that matches the standalone case. This observation is consistent across all scenarios B, C, and D. Nevertheless, a FCFS scheduling policy results in an increased deadline violation rate. For scenarios C and D, the deadline violation rates is 57.65% on average when applying a FCFS strategy. Under the FCFS-AOT policy in scenario C, the LLM achieves TTFT and TPT performance comparable to the (scenario A) but with a 62.6% deadline violation rate. Switching to FCFS-DYN that dynamically schedule layers on the best available HW decreases the deadline violation rate to 39.9%. As shown in Table 6, the deadline violation rate of SR-60 and Seg models significantly decreased to 0.5% and 0.0% respectively when applying dynamic scheduling. Nevertheless, the deadline violation rate of SR-120 increases to 77.4%, as well as the LLM’s TPT increases by 25.5% in scenario C under FCFS-DYN. For scenario D, we observe that applying FCFS-DYN does not reduce the deadline rate which remains at 66.5%, but increases the TPT by 86.9%. We observe in Table 6 that applying dynamic HW selection on scenario D shifted the deadline violations from the Seg model to the OD model. Therefore, utilizing FCFS to schedule *RTGEN* workloads leads to high deadline violation

rates (57.6% on average). While dynamic scheduling might limit the deadline violation problem, it is scenario and model dependent and can result in an increase in TPT.

GenAI Aware. Despite showing promising TTFT and TPT, FCFS schedulers fail to account for the real-time requirements of *RTGEN* workloads. Similarly, EDF policies cannot accommodate the long latencies of the generative LLMs. Therefore, *RTGEN* workloads require dynamic schedulers that are both real-time and generative AI aware. We observe that our simple heterogeneous policy FTF does not starve the LLM, achieves a TTFT that matches the standalone performance, and has a lower average deadline violation rate than FCFS. For scenarios B, C, and D, the TTFT is respectively 127.4 ms, 1577.9 ms, and 1577.9 ms matching the standalone scenario when running under FTF.

By assigning high priority to the first token generation, the FTF scheduler leverages the heterogeneous SoC to avoid EDF’s repeated preemption of the LLM and schedule the inference while still meeting real-time constraints for other models. This is possible because FTF explicitly treats the LLM’s TTFT as a high-priority deadline, preventing preemption during the prefill stage. Such prioritization is necessary due to the large gap between LLM layer latencies and the frame durations of real-time models, e.g., 98.6 ms vs. 16.7 ms in scenario C, which makes the LLM particularly vulnerable to starvation under standard EDF. In contrast, during the decode stage, the LLM’s per-layer latency becomes more comparable to that of other models, allowing for more balanced scheduling without excessive preempting under a conventional EDF.

Under FTF, the deadline violation rates of scenarios C and D decreases by 47.8% on average compared to FCFS. Nevertheless, the TPT significantly increases under FTF compared to the standalone case. The TPT of scenario C increases by 5.7 \times , and that of scenario D by 7.4 \times . The increase in TPT results in an increase in the decode stage and end-to-end latencies of the LLM inference especially as the number of generated tokens increases. These results further emphasize the importance of a workload-aware scheduler that can dynamically adapt to balance real-time constraints, multi-modality, and the long, input-dependent latencies of generative models.

5.2.2. Impact of the Sequence Length. As discussed in Section 2.2, *RTGEN* workloads can involve dynamic tensor shapes. Varying input prompt lengths in LLMs represent a form of tensor shape dynamicity common in generative workloads. Therefore we study how tensor shape dynamicity affect the scheduling of *RTGEN* workloads. We simulate scenario D with varying sequence lengths and list the results in Figure 6. The results in Figure 6 (a) indicate an increase in the deadline violation rate under the FTF scheduler from 1.7% for an input sequence of 32 tokens to 10.7% for an input of 2048 tokens. As we increase the input sequence length, the prefill latency increases as Figure 5 shows. Consequently, the LLM is occupying the available resources, the NPU in this case, for a longer time which

prevents other models from being scheduled and leads to deadline violations.

In addition, we observe an increase in TPT across all sequence lengths compared to the standalone case. This increase is caused by two primary factors. First, a portion of the decode layers are executed on the NPU, which is not the preferred backend for this stage. As shown in Figure 5, the NPU is $7.5\times$ slower than the GPU for decode operations, leading to a substantial increase in total inference time. Second, the increase is further exacerbated by additional waiting times in the inference queues due to backend contention.

More interestingly, we find that the TPT for 32- and 64-token inputs falls within the same range as the TPT for 2048-token inputs. This observation is unexpected, as TPT typically increases with context length. However, in this case, the high TPT for short sequences stems from aggressive offloading of decode layers to the NPU. Specifically, 95.1% of decode layers for the 32- and 64-token inputs are dispatched to the NPU, as shown in Figure 7. In contrast, for longer sequence lengths, only 37.4% of decode layers are executed on the NPU on average. This difference is attributed to the latency variability introduced by the input-dependent prefill stage, which affects backend availability at scheduling time. Based on these observations, we further motivate the need for a workload-aware dynamic scheduler that accounts for the dynamic execution behavior of generative models.

Summary. Our case studies highlight the performance heterogeneity of *RTGEN* workloads and the need for intelligent scheduling on heterogeneous systems. We show that preferred backends vary across models and even within different stages of a single model, as is the case with generative LLMs. This behavior is further complicated by dynamic input shapes, which shift backend suitability during runtime. We find that conventional scheduling policies such as EDF and FCFS fail to balance the conflicting demands of low-latency token generation and real-time deadline compliance. While FCFS improves LLM TTFT and TPT, it does so at the cost of high deadline violation rates. EDF policies, on the other hand, prioritize real-time models but starve the LLM entirely. Our GenAI-aware FTF scheduler strikes a better balance, achieving standalone-like TTFT with reduced deadline violations, but introduces higher TPT due to backend contention and decode-stage bottlenecks. We also demonstrate that input sequence length significantly impacts scheduling behavior, revealing that shorter sequences can suffer disproportionately due to resource contention and backend assignment. These findings underscore the need for a workload-aware scheduler that dynamically adapts to input characteristics, model stage, and system heterogeneity to meet the diverse demands of *RTGEN* workloads.

6. Related Works

LLM Scheduling. Many existing scheduling works [13, 14, 18, 37] optimize the deployment of generative LLMs.

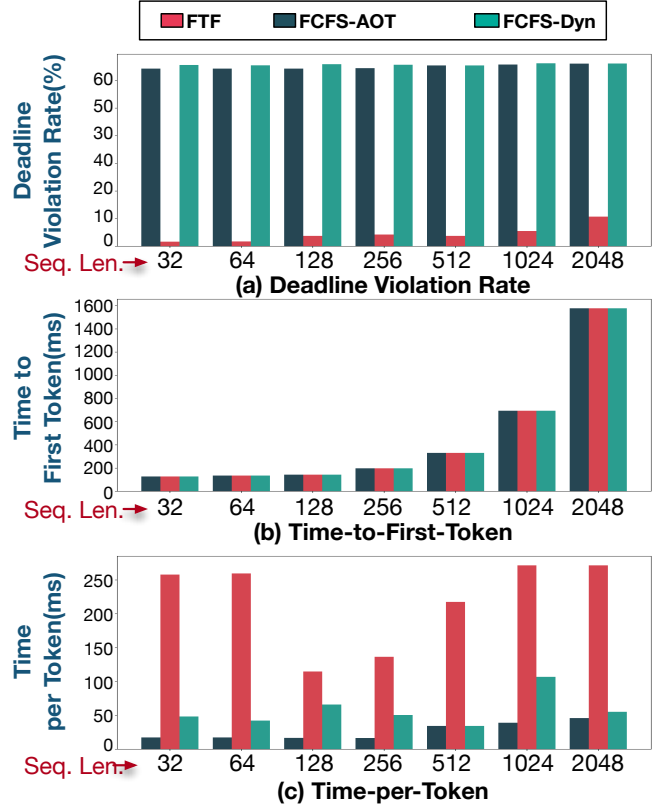


Figure 6: The impact of the input sequence length on the deadline violation rate, time-to-first-token, and time-per-token of scenario D.

Flexgen [37] proposes a throughput oriented schedule to enable running LLMs on a single GPU with limited memory. Flexgen statically partitions the layers of LLMs across CPU and GPU memory, and schedules the GPU computations to maximize weight reuse. Nevertheless, Flexgen does not account for the multi-model inference scenarios, which makes its static scheduling approach unsuitable for emerging workloads, described in Section 3, that concurrently running LLMs with real-time models. NeuPIMS [13] proposes a heterogeneous architecture that integrates NPUs with processing in memory cores (PIMs) to accelerate batched generative LLM inference. NeuPIMS scheduler partitions the batches into sub-batches to parallelize the execution of the multi-head attention layer across the heterogeneous backend. Nonetheless, NeuPIMS only focuses on LLM serving and does not investigate the LLM inference scheduling problem in a real-time multi-model settings. Unlike previous works [13, 14, 18, 37], our work studies the performance of generative LLM inference on heterogeneous systems in real-time application scenarios. We evaluate the importance of the scheduling policy in managing the challenges of real-time generative multi-model workloads.

Scheduling on Heterogeneous Systems. Previous works [8, 11, 15, 16] investigate the scheduling problem on heterogeneous systems. However, their characterization

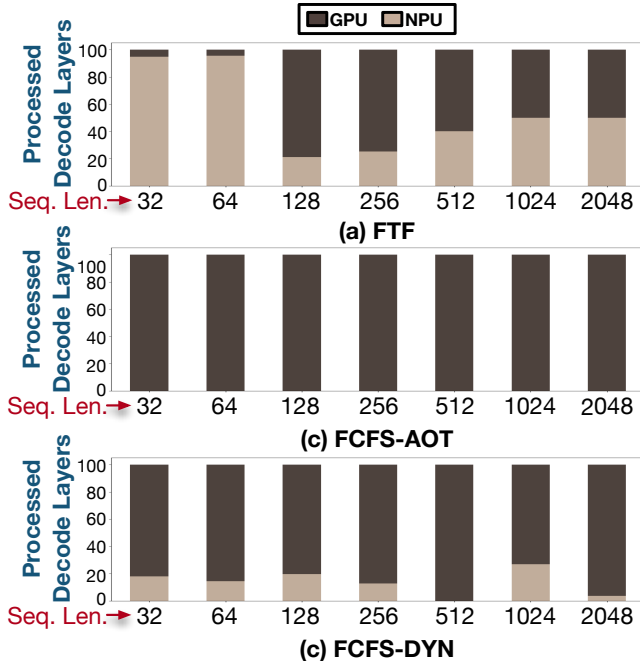


Figure 7: The percentage of LLM layers processed on the GPU and NPU during 32 decode iterations for the video conference scenario (scenario D in Table 2).

TABLE 5: THE IMPACT OF VARIOUS SCHEDULING POLICIES FROM TABLE 4 ON THE DEADLINE VIOLATION RATE, TIME-TO-FIRST-TOKEN (TTFT), AND TIME PER TOKEN (TPT) OF THE WORKLOAD SCENARIOS DEFINED IN TABLE 2.

Scenario	Scheduler	Performance Metrics		
		Deadline Viol. Rate(%)	Time to First Token(ms)	Time per Token(ms)
Scenario A	EDF-AOT	-	1577.9	45.9
	EDF-Dyn	-	1577.9	45.9
	FCFS-AOT	-	1577.9	45.9
	FCFS-Dyn	-	1577.9	45.9
	FTF	-	1577.9	45.9
Scenario B	EDF-AOT	0.0	-	-
	EDF-Dyn	0.0	-	-
	FCFS-AOT	0.3	127.4	39.0
	FCFS-Dyn	0.0	127.4	39.0
	FTF	0.0	127.4	39.0
Scenario C	EDF-AOT	0.0	-	-
	EDF-Dyn	0.0	-	-
	FCFS-AOT	62.6	1577.9	45.9
	FCFS-Dyn	39.9	1577.9	61.6
	FTF	44.4	1577.9	263.1
Scenario D	EDF-AOT	0.0	-	-
	EDF-Dyn	0.0	-	-
	FCFS-AOT	66.5	1577.9	84.0
	FCFS-Dyn	66.5	1577.9	85.8
	FTF	20.8	1577.9	339.9

and approach focus on a limited set of workloads [8] or a specific class of backend [15]. DREAM [15] is a state-of-the-art dynamic scheduler tailored for real-time multi-model (RTMM) workloads. DREAM quantifies the requirements of RTMM workloads into metrics which are used to drive the scheduling decision. It employs tunable

TABLE 6: THE DEADLINE VIOLATION RATE PER MODEL FOR SCENARIOS C AND D.

Scenario	Models	Schedulers		
		FCFS-AOT	FCFS-DYN	FTF
Gaming II	SR-120	53.1%	77.4%	8.3%
	SR-60	99.5%	0.5%	95.8%
	Seg	46.5%	0.0%	69.8%
Video Conference	SR	99.4%	99.5%	16.1%
	Seg	46.5%	0.0%	0.0
	OD	53.9%	99.5%	16.1%

parameters to effectively adapt to the workload’s dynamicity. In addition, DREAM focus on RTMM workloads based on AR/VR applications running on heterogeneous dataflow accelerator backend. Our work extends on these efforts by analyzing the impact of scheduling on a new class of emerging models integrating RTMM with generative models deployed on NPU-GPU systems. Map and Conquer [8] offers an optimization framework to statically partition and schedule single model neural network inference on GPU-NPU systems. Because the proposed approach is tailored to single model inference, it does not account for the dynamic change in resource availability that results from multi-model workloads. Our work motivates the need for a dynamic scheduler when running real-time generative workloads.

7. Conclusion

The emergence of *RTGEN* workloads poses significant challenges for on-device execution. While heterogeneous SoCs’ characteristics seem very promising for such emerging workloads, their scheduling space is exponentially large. In this work, we explore the impact of the scheduling on the performance horizon of emerging *RTGEN* workloads. We define four realistic scenarios and thoroughly characterize their performance under five scheduling policies. Our study shows that the scheduling policy significantly affects the deadline violation rate, TTFT, and TPT of the *RTGEN* scenarios, and it motivates the need for workload-aware scheduling strategies that can dynamically adapt to backend availability, model heterogeneity, and the characteristics of *RTGEN* workloads.

References

- [1] Josh Achiam, Steven Adler, Sandhini Agarwal, Lama Ahmad, Ilge Akkaya, Florencia Leoni Aleman, Diogo Almeida, Janko Altschmidt, Sam Altman, Shyamal Anadkat, et al. Gpt-4 technical report. *arXiv preprint arXiv:2303.08774*, 2023.
- [2] Advanced Micro Devices, Inc. AMD FidelityFX Super Resolution. <https://www.amd.com/en/products/graphics/technologies/fidelityfx/super-resolution.html>.
- [3] Advanced Micro Devices, Inc. AMD Radeon texttrademark RX ,7900 ,XTX graphics card. <https://www.amd.com/en/products/graphics/desktops/radeon/7000-series/amd-radeon-rx-7900xtx.html>.
- [4] Advanced Micro Devices, Inc. AMD Ryzen™ AI – Windows PCs with AI Built In. <https://www.amd.com/en/products/processors/consumer/ryzen-ai.html>.

- [5] AMD. RyzenAI-SW: AMD Ryzen™ AI Software. <https://github.com/amd/RyzenAI-SW>.
- [6] Apple Inc. Apple reveals M3 Ultra, taking Apple silicon to a new extreme. <https://www.apple.com/newsroom/2025/03/apple-reveals-m3-ultra-taking-apple-silicon-to-a-new-extreme/>, Oct 2023.
- [7] Akari Asai, Zeqiu Wu, Yizhong Wang, Avirup Sil, and Hannaneh Hajishirzi. Self-rag: Learning to retrieve, generate, and critique through self-reflection. In *The Twelfth International Conference on Learning Representations*, 2023.
- [8] Halima Bouzidi, Mohamad Odema, Hamza Ouarnoughi, Smail Niar, and Mohammad Abdullah Al Faruque. Map-and-conquer: Energy-efficient mapping of dynamic neural nets onto heterogeneous mpsoes. In *2023 60th ACM/IEEE Design Automation Conference (DAC)*, pages 1–6. IEEE, 2023.
- [9] Alexey Dosovitskiy, Lucas Beyer, Alexander Kolesnikov, Dirk Weissenborn, Xiaohua Zhai, Thomas Unterthiner, Mostafa Dehghani, Matthias Minderer, G Heigold, S Gelly, et al. An image is worth 16x16 words: Transformers for image recognition at scale. In *International Conference on Learning Representations (ICLR)*, 2020.
- [10] Roberto Gallotta, Graham Todd, Marvin Zammit, Sam Earle, Antonios Liapis, Julian Togelius, and Georgios N Yannakakis. Large language models and games: A survey and roadmap. *IEEE Transactions on Games*, 2024.
- [11] Soroush Ghodrati, Byung Hoon Ahn, Joon Kyung Kim, Sean Kinzer, Brahmendra Reddy Yatham, Navateja Alla, Hardik Sharma, Mohammad Alian, Eiman Ebrahimi, Nam Sung Kim, et al. Planaria: Dynamic architecture fission for spatial multi-tenant acceleration of deep neural networks. In *2020 53rd Annual IEEE/ACM International Symposium on Microarchitecture (MICRO)*, pages 681–697. IEEE, 2020.
- [12] Aaron Grattafiori, Abhimanyu Dubey, Abhinav Jauhri, Abhinav Pandey, Abhishek Kadian, Ahmad Al-Dahle, Aiesha Letman, Akhil Mathur, Alan Schelten, Alex Vaughan, et al. The llama 3 herd of models. *arXiv preprint arXiv:2407.21783*, 2024.
- [13] Guseul Heo, Sangyeop Lee, Jaehong Cho, Hyunmin Choi, Sanghyeon Lee, Hyungkyu Ham, Gwangsun Kim, Divya Mahajan, and Jongse Park. Neupims: Npu-pim heterogeneous acceleration for batched llm inferencing. In *Proceedings of the 29th ACM International Conference on Architectural Support for Programming Languages and Operating Systems, Volume 3*, pages 722–737, 2024.
- [14] Keisuke Kamahori, Tian Tang, Yile Gu, Kan Zhu, and Baris Kasicki. Fiddler: Cpu-gpu orchestration for fast inference of mixture-of-experts models. *arXiv preprint arXiv:2402.07033*, 2024.
- [15] Seah Kim, Hyoukjun Kwon, Jinook Song, Jihyuck Jo, Yu-Hsin Chen, Liangzhen Lai, and Vikas Chandra. Dream: A dynamic scheduler for dynamic real-time multi-model ml workloads. In *Proceedings of the 28th ACM International Conference on Architectural Support for Programming Languages and Operating Systems, Volume 4*, pages 73–86, 2023.
- [16] Hyoukjun Kwon, Liangzhen Lai, Michael Pellauer, Tushar Krishna, Yu-Hsin Chen, and Vikas Chandra. Heterogeneous dataflow accelerators for multi-dnn workloads. In *2021 IEEE International Symposium on High-Performance Computer Architecture (HPCA)*, pages 71–83. IEEE, 2021.
- [17] Hyoukjun Kwon, Krishnakumar Nair, Jamin Seo, Jason Yik, Debabrata Mohapatra, Dongyuan Zhan, Jinook Song, Peter Capak, Peizhao Zhang, Peter Vajda, et al. Xrbench: An extended reality (xr) machine learning benchmark suite for the metaverse. *Proceedings of Machine Learning and Systems*, 5:1–20, 2023.
- [18] Wonbeom Lee, Jungi Lee, Junghwan Seo, and Jaewoong Sim. {InfiniGen}: Efficient generative inference of large language models with dynamic {KV} cache management. In *18th USENIX Symposium on Operating Systems Design and Implementation (OSDI 24)*, pages 155–172, 2024.
- [19] Patrick Lewis, Ethan Perez, Aleksandra Piktus, Fabio Petroni, Vladimir Karpukhin, Naman Goyal, Heinrich Küttler, Mike Lewis, Wen-tau Yih, Tim Rocktäschel, et al. Retrieval-augmented generation for knowledge-intensive nlp tasks. *Advances in neural information processing systems*, 33:9459–9474, 2020.
- [20] Zehan Li, Xin Zhang, Yanzhao Zhang, Dingkun Long, Pengjun Xie, and Meishan Zhang. Towards general text embeddings with multi-stage contrastive learning. *arXiv preprint arXiv:2308.03281*, 2023.
- [21] Jamie Menjay Lin, Siargey Pisarchyk, Juhyun Lee, David Tian, Tingbo Hou, Karthik Raveendran, Raman Sarokin, George Sung, Trent Tolley, and Matthias Grundmann. Efficient heterogeneous video segmentation at the edge. *arXiv preprint arXiv:2208.11666*, 2022.
- [22] Ji Lin, Jiamei Tang, Haotian Tang, Shang Yang, Wei-Ming Chen, Wei-Chen Wang, Guangxuan Xiao, Xingyu Dang, Chuang Gan, and Song Han. Awq: Activation-aware weight quantization for on-device llm compression and acceleration. *Proceedings of Machine Learning and Systems*, 6:87–100, 2024.
- [23] Ze Liu, Yutong Lin, Yue Cao, Han Hu, Yixuan Wei, Zheng Zhang, Stephen Lin, and Baining Guo. Swin transformer: Hierarchical vision transformer using shifted windows. In *Proceedings of the IEEE/CVF international conference on computer vision*, pages 10012–10022, 2021.
- [24] Camillo Lugaresi, Jiuqiang Tang, Hadon Nash, Chris McClanahan, Esha Uboweja, Michael Hays, Fan Zhang, Chuo-Ling Chang, Ming Guang Yong, Juhyun Lee, et al. Mediapipe: A framework for building perception pipelines. *arXiv preprint arXiv:1906.08172*, 2019.
- [25] Microsoft. AI Tools for Organizations | Microsoft Copilot. <https://www.microsoft.com/en-us/microsoft-copilot/organizations>.
- [26] Microsoft. Virtual Meeting Backgrounds and Background Blur | Teams. <https://www.microsoft.com/en-us/microsoft-teams/virtual-meeting-backgrounds>.
- [27] Microsoft. microsoft/onnxruntime-genai: Generative ai extensions for onnx runtime. <https://github.com/microsoft/onnxruntime-genai>, 2021.
- [28] Naba Kumar. Enhancing Teams Video Quality with Super Resolution. <https://techcommunity.microsoft.com/blog/microsoftteamsblog/enhancing-teams-video-quality-with-super-resolution/4373307>, Feb 2025.
- [29] ONNX Runtime. Vitis AI Execution Provider. <https://onnxruntime.ai/docs/execution-providers/Vitis-AI-ExecutionProvider.html>.
- [30] ONNX Runtime. Windows - DirectML Execution Provider. <https://onnxruntime.ai/docs/execution-providers/DirectML-ExecutionProvider.html>.
- [31] Joon Sung Park, Joseph O’Brien, Carrie Jun Cai, Meredith Ringel Morris, Percy Liang, and Michael S Bernstein. Generative agents: Interactive simulacra of human behavior. In *Proceedings of the 36th annual acm symposium on user interface software and technology*, pages 1–22, 2023.
- [32] Qualcomm Inc. Laptops, Desktops & Tablets | Snapdragon. <https://www.qualcomm.com/products/mobile/snapdragon/pcs>.
- [33] Qualcomm Technologies, Inc. Best AI PCs: Exploring the Next Generation of Computing. <https://www.qualcomm.com/snapdragon/laptops-and-tablets/best-ai-pcs>.
- [34] Mariam Rakka, Jinhao Li, Guohao Dai, Ahmed Eltawil, Mohammed E Fouda, and Fadi Kurdahi. Softmap: Software-hardware co-design for integer-only softmax on associative processors. In *2025 Design, Automation & Test in Europe Conference (DATE)*, pages 1–7. IEEE, 2025.
- [35] Joseph Redmon and Ali Farhadi. Yolov3: An incremental improvement. *arXiv preprint arXiv:1804.02767*, 2018.
- [36] ONNX Runtime developers. Onnx runtime. <https://onnxruntime.ai/>, 2021.

- [37] Ying Sheng, Lianmin Zheng, Binhang Yuan, Zhuohan Li, Max Ryabinin, Beidi Chen, Percy Liang, Christopher Ré, Ion Stoica, and Ce Zhang. Flexgen: High-throughput generative inference of large language models with a single gpu. In *International Conference on Machine Learning*, pages 31094–31116. PMLR, 2023.
- [38] Streamlabs. Introducing Streamlabs’ New Intelligent Streaming Assistant in Collaboration with NVIDIA and Inworld AI. <https://streamlabs.com/content-hub/post/introducing-streamlabs-new-intelligent-streaming-assistant-in-collaboration-with-nvidia-and-inworld-ai>, Jan 2025.
- [39] Dani Valevski, Yaniv Leviathan, Moab Arar, and Shlomi Fruchter. Diffusion models are real-time game engines. *arXiv preprint arXiv:2408.14837*, 2024.
- [40] Ashish Vaswani, Noam Shazeer, Niki Parmar, Jakob Uszkoreit, Llion Jones, Aidan N Gomez, Lukasz Kaiser, and Illia Polosukhin. Attention is all you need. *Advances in neural information processing systems*, 30, 2017.
- [41] Sourabh Vora, Alex H Lang, Bassam Helou, and Oscar Beijbom. Pointpainting: Sequential fusion for 3d object detection. In *Proceedings of the IEEE/CVF conference on computer vision and pattern recognition*, pages 4604–4612, 2020.
- [42] Susan Zhang, Stephen Roller, Naman Goyal, Mikel Artetxe, Moya Chen, Shuohui Chen, Christopher Dewan, Mona Diab, Xian Li, Xi Victoria Lin, et al. Opt: Open pre-trained transformer language models. *arXiv preprint arXiv:2205.01068*, 2022.
- [43] Yulun Zhang, Kungpeng Li, Kai Li, Lichen Wang, Bineng Zhong, and Yun Fu. Image super-resolution using very deep residual channel attention networks. In *Proceedings of the European conference on computer vision (ECCV)*, pages 286–301, 2018.
- [44] Zoom Video Communications, Inc. Using blurred background – Zoom. https://support.zoom.com/hc/en/article?id=zm_kb&sysparm_article=KB0061066.
- [45] Zoom Video Communications, Inc. Using gesture recognition – Zoom. https://support.zoom.com/hc/en/article?id=zm_kb&sysparm_article=KB0067842.
- [46] Zoom Video Communications, Inc. Zoom AI Assistant. <https://www.zoom.com/en/products/ai-assistant/>.